Free Wake Techniques For Rotor Aerodynamic Analyses. Vol. I : Summary of Results + Background

R.H. Miller.

NASA-CR-166434
19830011440

A Reproduced Copy

OF

NASA-CR-166,434

NASA CONTRACTOR REPORT 166434

Free Wake Techniques for Rotor Aerodynamic Analysis; Volume No. I - Summary of Results and Background Theory

R. H. Miller

CONTRACT NAG2-47
December 1982

NASA

NASA CONTRACTOR REPORT 166434

Free Wake Techniques for Rotor Aerodynamic Analysis; Volume No. I - Summary of Results and Background Theory

R. H. Miller
Department of Aeronautics and Astronautics
Massachusetts Institute of Technology
Cambridge, Massachusetts

Prepared for Ames Research Center under
NASA Cooperative Agreement No. NAG2-47

National Aeronautics and
Space Administration

Ames Research Center
Moffett Field, California 94035

TABLE OF CONTENTS

NOMENCLATURE

C_T	thrust cofficient = $T/\rho S\Omega^2R^2$
E	elliptic integral of the second kind
K	elliptic integral of the first kind
R	rotor radius
S	rotor disc area = πR^2
T	rotor thrust
b	blade chord
k	modulus of elliptic integral
p	distance between airfoils
r	radial location of originating vortex nondimensionalized by R
u	radial component of induced velocity
v	axial component of induced velocity at actuator disc
w	axial component of induced velocity
ws	self induced velocity on curved vortex
z	vertical distance nondimensionalized by R
Γ	circulation
Δr	vortex core radius
Ω	rotational speed, sec^{-1}
γ	distributed vorticity on blade
η	radial station at which induced velocity is desired nondimensionalized by
λ	inflow ratio, $w/\Omega R$
ψ,Ψ	azimuth of any point relative to blade

SUMMARY

This report is volume I of a three volume series entitled "Free Wake Techniques for Rotor Aerodynamic Analysis" and covering the following topics:

Volume I (present volume) "Summary of Results and Background Theory" reviews the results obtained to date using both complete and simplified wake models and summarizes the theoretical background on which these models are based.

Volume II "Vortex Sheet Models" (Ref. 5) presents the results of computations using complete and modified vortex sheet models and tests the sensitivity of the solutions to various assumptions used in the development of the models. The complete codings are included.

Volume III "Vortex Filament Models" (Ref. 6) discusses results obtained using a vortex filament model, as opposed to sheets, again using various modelling techniques and including the computer codings.

SECTION I INTRODUCTION

This report will discuss results obtained to date during the development of a consistent aerodynamic theory for rotors in hovering flight. Methods of aerodynamic analysis have been developed which are adequate for general design purposes until such time as more elaborate solutions become available, in particular solutions which include real fluids effects. It is recognized that such solutions are not yet within the capability of even the most powerful computational facilities. Nevertheless it is hoped that continued research, both experimental and computational, will lead to further definition of the real fluids problem and narrow the range of empiricism now required to handle these effects.

Several problems were encountered in the course of this development, and many remain to be solved, however it is felt that a better understanding of the aerodynamic phenomena involved has been obtained. Remaining uncertainties are discussed in the following sections and in the companion volumes (Refs. 5 and 6) covering this study.

Experimental investigations (Refs. 1, 2, 3, 4) have shown that the wake geometry of a hovering rotor differs appreciably from the simple spiral form of constant diameter assumed in classical theory. The airload distribution on a rotor blade is critically dependent on this geometry and particularly on the distance between the blade and the tip vortex generated by the previous blade at their first encounter, as indicated in Fig. 1, and on the structure of the vortex at this encounter. There is strong experimental evidence that this vortex, trailed initially from the blade as the bound circulation drops rapidly from a peak at about 90% of rotor span to the tip, rolls up rapidly into a tight and strong tip vortex whose strength is close to the maximum strength of the bound circulation on the rotor blade. What is not known is

the azimuth locations over which this roll up occurs, the structure of the resultant vortex core and the mutually induced velocities in the near wake during the roll up process. These velocities are important in determining the vertical location of the vortex at first encounter.

It is convenient to consider the wake as divided into three segments. The first segment, the near wake, contains that portion of the wake attached to a particular blade and before first encounter with a following blade. The second segment, the intermediate wake, includes the wake from the first encounter through two or more spirals. The third segment, the far wake, contains the rest of the wake to infinity. It is generally a reasonable approximation to treat only the first two segments of the wake as free, that is with a geometry determined by the induced velocities in the wake, and to consider the far wake as a vortex cylinder of constant radius and strength determined by the radius and vortex spacing at the end of the intermediate wake. Calculation of the intermediate and far wake geometries requires extensive computational capabilities, but otherwise present no serious problem. There is some question as to the suitability of using a fixed geometry far wake, as discussed in section IV, however, as might be expected, assumptions relating to the far wake do not appear to have a major impact on the solutions.

Of more concern is the treatment of the near wake. Figure 2 shows a typical spanwise distribution of bound circulation on a two-bladed rotor from both the experimental results of Ref. 4 and the analytical results of Ref. 7. The rapid drop off of circulation over the outer portion of the blade results in a trailing wake system which may be modelled mathematically as a series of curved vortex filaments as shown in Fig. 3. The induced velocities acting on this system of vortex filaments from the far and intermediate wakes can

be readily determined given the wake geometry. However it is primarily the mutually induced velocities due to the near wake which determines the roll up process and hence the eventual near wake displacements.

In section II of this report various models are discussed for determining the near wake displacements and it is shown that reasonable agreement with experimental results are obtained with versions of the following three models

a) A model in which the near and intermediate wakes are represented by spiral vortex sheets which are assumed to roll up following various schedules (Ref. 5)

b) A model in which the wake is represented by spiral vortex filaments (Ref. 6)

c) A simplified model in which the wake is represented by either vortex rings or doubly infinite line vortices (Ref. 7)

Section III examines the roll up process of the tip vortex in greater detail and presents an alternate treatment of the entire near wake and its roll up process with suggestions for a more elaborate approach to the problem.

Section IV briefly discusses far wake effects and shows the dependence of wake geometry on the persistence of circulation in the far wake.

Section V presents the background theory used in the development of the various wake models.

Section VI summarizes conclusions from this study and presents recommendations for further investigations.

SECTION II VORTEX WAKE MODELS

The various wake models and their evolution to the final version using a combination of vortex sheets and vortex filaments are discussed in detail in Refs. 5 and 6 which form Volume II and III of the present series. The first wake model used was originally developed in Ref. 8 for the treatment of wind turbine wakes. The same model was applied to a hovering helicopter rotor and preliminary results using this program were presented in Refs. 9 and 10. Ref. 9 reported progress at midpoint in the original contract schedule, comparing results using the original program with the experimental data of Refs. 2, 11 and 12. Discrepancies were noted and plans for future research outlined. Ref. 10 reported progress at a later point in the contract schedule, and included results from the first two of five free vortex models developed during the course of the investigation. The vortex sheet models of Ref. 10 contained an inadvertent doubling of the strength of the far wake which resulted in a small error, corrected in the later models discussed in Ref. 5. Again, discrepancies with the experimental results were noted which were attributed to the termination of the vortex sheets in less than one spiral. Attempts to extend the solution beyond 360° were unsuccessful because of lack of convergence. The solution was based on iteration of the wake geomet , which required an appreciable amount of CPU time due to the complexity of the distorting vortex sheet model. The problem with convergence was believed due to the roll up of the vortex sheet which was not being properly modelled because of the coarseness of the mesh required to keep CPU time to manageable proportions, of the order of an hour.

The four vortex sheet models developed in Volume II may be summarized

as follows:

MODEL 1 Essentially the same as Ref. 8, in which the near and intermediate wakes are represented by a segmented vortex sheet connecting a tip and root vortex. The far wake is represented by vortex cylinders as in Ref. 7.

MODEL 2 The near wake is treated as in Model 1 until an azimuth of $\phi = 255°$, after which it is rolled up into three vortex filaments as in Ref. 7. The location of these filaments at $\phi = 255°$ is determined as if the filaments had rolled up immediately at $\phi = 0$.

MODEL 3 Same as Model 2, except that the near wake is rolled up before first encounter, at $\phi = 45°$, and is assumed to remain in the rotor plane until roll up. The geometry of the rolled up vortices at $\phi = 45°$ is determined as in Model 2. This avoids the lengthy computations required to establish the geometry of the vortex sheets and hence is computationally much more efficient than Model 2.

MODEL 4 Same as Model 3, except that the full vortex sheet model, including tip and root vortices, is used to establish the geometry of the vortex filaments at roll up.

In addition a filamentary wake model, Model 5, was developed as discussed in Volume III, Ref. 6.

MODEL 5 The filamentary near wake is allowed to roll up as in Model 2, but to $\phi = 70°$, after which the centroid of the partially rolled up wake is used to describe the wake geometry. The roll up process is similar to that of the Model 2 vortex sheets shown in Fig. 4.

The continuing investigations discussed in Section III indicate that the roll up with a more finely modelled near wake with trailing filaments located approximately every .3% span at the tip would be much faster than with the relatively coarse mesh size with a minimum spacing of 2% of the span used with the vortex sheet model. The roll up predicted by the vortex sheet model at the first intersection (180°) is shown in Fig. 4. Although the start of roll up is clearly evident, it is not nearly as tight as predicted by the finer mesh model of Section III as shown in Fig. 10. The location of the tip vortex close to but above the blade most probably caused the oscillatory divergence of the solution.

In the meantime, a separate investigation had been conducted in which attempts were made to develop a simplified model of the wake which could be used to aid in clarifying the physics of the problem. This investigation resulted in the development of the analytical technique described in detail in Ref. 7, with later results appearing in Refs. 13 and 14. The simplified program is capable of predicting wake geometry and air loads in a few seconds of CPU time and with reasonable accuracy. Velocities are computed in the wake immediately behind each blade only, and these velocities are averaged in order to obtain wake displacements. The averaging process in the near wake was based on experience with the more complete solution (see page 8 and Fig. 7) and avoids the need for computation of the wake displacements during the roll up process.

Some of the results obtained with the simplified model are shown in Fig. 2. The computed results are in reasonable agreement with test data as regards bound circulation distribution and geometry. Some discrepancies exist in the region of the drop off of circulation near the

80% span point for reasons which are not clear but which are believed to be associated with the spanwise flow and real fluids effects discussed in Ref. 14 and in Section III.

The simple model was based on the assumption that the trailing wake of the blade rolled up almost immediately according to the Betz criteria of conservation of angular and linear momenta (Ref. 7) and only the rolled up wake need be considered in the intermediate and far wakes. The near wake was treated as a relatively fine series of semi-infinite vortex filaments extending from the blade and was used only in determining the bound circulation distribution on the blade itself in the presence of induced velocities from the rolled up vortices. Fig. 5 indicates schematically the simplified wake model. The velocities induced by the vortex rings and cylinders could be expressed as elliptical integrals amenable to rapid series solution, consequently CPU time was kept to a minimum.

simplified wake analysis

In view of the success of the simplified model it was decided to use a similar roll up schedule for the more detailed models. The vortex sheets were therefore rolled up, again according to the Betz criteria, at various points in the near wake thereby avoiding the problems with the slow roll up predicted by the coarse meshed model discussed above. Volume II (Ref. 5) contains a detailed discussion of the various attempts to obtain satisfactory results with this model. Typical final results (Fig. 6) show reasonable agreement with test data.

It became evident in the development of this revised vortex sheet model that a problem existed in determining the local velocities contributing to the displacement of the tip vortex, either rolled up or in sheet form, between its generation by one blade and encounter with the following blade. The rolled up tip vortex is located at approximately

97.5% of the span and the computed velocities at the blade tip and at 95% span typically are as shown in Fig. 7. One possibility would be to average the velocities at these two stations giving the results shown by the heavy line in Fig. 7. This was the basis for adopting the averaging process in the simplified solution of Ref. 7 and in Ref. 5 as a reasonable approximation for determining the position of the rolled up tip vortex at first encounter. However such treatment of the tip vortex is an approximation only and not necessarily the true mechanism determining its migration in the near wake.

In an attempt to obtain a clearer understanding of these problems, Model 5 was developed as described in Ref. 6 with the wake represented by vortex filaments rather than vortex sheets. The original vortex sheet model was developed on the basis of experience with an earlier filamentary wake model developed in Ref. 15 for the forward flight case where it was found that a better representation of blade loads could be obtained if the wake at first encounter were represented by a vortex sheet rather than a concentrated curved vortex. However, in hovering flight, and at least for the two bladed case, the vortex at first encounter is sufficiently far below the blade so that the filamentary representation of the wake is adequate. Certainly the computational difficulties encountered in matching the edges of the segments of the distorting sheets are avoided.

Results from the filamentary model are discussed in detail in Vol. III (Ref. 6), together with conclusions as to its limitations and that of the other models. The predicted wake geometry agrees well with the experimental data although the previously noted dip in bound circulation near 80% span persists and requires somewhat arbitrary assumptions as to core size to improve agreement with test data.

It should be noted that the change in lift at the 80% span may be sufficiently rapid to trigger separation of the type first noted in Ref. 16,

and discussed in Ref. 14, when a close blade/vortex encounter occurs. Furthermore, there exists at the 80% span a wake induced radial velocity of the order of 10% of the tangential velocity due to blade rotation. The flow will therefore approach the blade at an angle of the order of 5° which will introduce further second order effects similar to the effects of sweep. A more complete lifting surface solution of the type discussed in Ref. 17, rather than a lifting line solution, is required in order to investigate such effects.

SECTION III VORTEX ROLL-UP

Recent interest in the formation of vortices from fixed wind aircraft has stimulated the development of computation techniques for predicting the geometries of rolled up three dimensional vortex sheets. In these techniques the sheet is treated as a collection of line or point vortices and their motions tracked as they distort under their mutual interference velocities using various computational methods. Some of the earliest work[18] is quoted in Ref. 19, pp. 589-590. Subsequent efforts to duplicate these results with a finer grid resulted in chaotic motions, particularly in the tighter portions of the spiral. Introduction of artificial viscosity resulted in more ordered solutions but, unfortunately, dependent on the degree of viscosity introduced.

Most recent efforts have concentrated on the Euler-Lagrange solutions in which a series of point vortices are tracked in a Lagrangian frame of reference and referred back to on Eulerian frame for solution of the equations of flow. This "cloud in cell" technique was applied to the roll up of vortex sheets from a wing in Ref. 20 and more recently in Ref. 21. In Ref. 22 the two dimensional approximation to the rotor wake developed in Ref. 7 was applied to the computation of the roll up of an assumed straight wake from a rotor blade as it descended in hovering flight. A typical solution is shown in Fig. 8 which clearly indicates the roll up process. Time did not permit completing the study to a converged solution. This work is being continued using the three dimensional model of Ref. 7 which allows for curvature in the wake. Preliminary work has concentrated on determining the effects of cell size as one measure of the degree of artificial viscosity introduced in the solution. Dependence of the solution on the assumed cell size remains a matter of concern.

In this section we will discuss a further approach to the problem of vortex sheet roll up in which the wake is modelled as a curved series of vortex filaments and their roll up predicted using the Biot-Savart relationships. In Ref. 6 the complete solution has been obtained for a series of spiral vortex filaments, but only a limited number of such filaments could be used in order to keep the CPU time reasonable. In this section the roll up of the near wake only will be considered and a simplified approach taken in order to minimize the required computer time and clarify the nature of the problem.

Referring to Fig. 9, it is necessary to compute interference velocities between any two vortex filaments everywhere in the first spiral and integrate these velocities to obtain displacement. If it is desired to compute the velocity induced at any point A by another vortex filament B, then it is is clear that the velocity at A due to B would be primarily due to that portion of B closest to A. The rest of the spiral vortex filament B may be approximated by a vortex ring and the velocities computed readily by the techniques discussed in Section V using the Biot-Savart relationships and logarithmic series solutions for the resulting elliptic integrals. The displacement of any vortex may be computed by integrating the total induced velocity on a vortex due to contributions from all other vortices in the near wake over an increment of time represented by a small change in azimuth, starting from the blade in question, using standard techniques of integration such as fourth order Runge/Kutta formulas. With this simplified model it is possible to set up a much finer wake structure, thereby presumably achieving a more realistic wake roll up.

This technique was first used to examine the roll up of the curved vortex generated from the tip of the blade using a fine distribution of filaments. A typical result is shown in Fig. 10. Nineteen filaments were

generated from the outer six percent of the blade with an assumed core size of 1% of blade span. Most of the vorticity is contained in the numbered vortex filaments and in particular the first six as is evident from the table showing the strength of each vortex filament, g, where g is equal to $\Gamma/\Omega R^2$ with a maximum value of .02 at 94% span. It may be deduced from Fig. 10 that the vortex rolls up very rapidly, first rising and then descending. Roll up apparently occurs a few chord lengths behind the rotor blade, as may be expected from the experimental evidence.

The vertical displacement of what is apparently the vortex core is characteristic of a curved vortex sheet and not a straight sheet. In the latter case, it may be shown that no vertical displacement of the centroid of vorticity will occur if the effect of blade bound vorticity on the wake is neglected.

The wake displacements due to the bound vorticity of one blade will, to first order, be cancelled by that of the following blade, resulting in no net displacement of the vortex filaments, whether curved or straight, due to bound circulation. Fig. 11 shows the displacement of a free vortex with and without the presence of bound vorticity computed using the analytical techniques discussed in Section V. The net effects are evidently small everywhere in the wake and essentially zero at the first encounter with the following blade. Consequently the bound circulation has not been included in the results of Fig. 10 in order to clarify the more important effects due to the mutually induced velocities of the free vorticities. It should be noted that the bound circulation is included in all the complete solutions discussed in Vols. II and III.

Two factors remain of concern in the roll up predictions: the step size used in the integration of velocity in order to obtain displacement and the

assumed vortex core size. The effect of core size on the displacement of the centroid of vorticity is shown in Fig. 12. Evidently the displacement is dependent on the assumed core size. When zero core size is used the results tend to become chaotic near the centroid of the spiral as previous investigators have found. Furthermore the solution becomes more sensitive to the interval size used in integration whereas this is not the case for a solution containing a sufficient amount of artificial viscosity as shown in Fig. 12.

For a two bladed rotor Fig. 2 indicates that the tip vortex at first encounter is located approximately 5 to 6% of the span below the following blade, as shown both analytically (Ref. 7) and experimentally (Ref. 4). Consequently, the differences in the vertical displacement of the centroid of the rolled up vortex with various assumptions as to core size, of the order of less than 1% of the blade span at first encounter, may not appear to be crucial. However blade airloads are sensitive to the location of the tip vortex at this first encounter and the dependency of the solution on assumption as to core size remains of some concern. Experimental evidence (Ref. 23) indicates vortex core sizes of the order of 1% of the span, but these measurements are presumably of the rolled up vortex core, which may not necessarily be the core size of the filaments which model the sheet as it leaves the blade. A great deal more analytical and experimental investigation is necessary before this problem may be completely resolved. It is possible that simplified forms of the Navier-Stokes equations for spiraling vortices will have to be developed in order to obtain a better understanding of the phenomenon of roll up and migration of the tip vortex generated by a rotating blade.

As a first attempt to extend this investigation to the complete wake, an approximate solution was obtained using 24 vortex filaments for the near wake. A converged solution was first obtained using the fast free wake

techniques of Ref. 7, where the near wake is assumed to roll up almost instantly. The resulting wake geometry was then used to predict the intermediate and far wake velocities at the blade and these were added to those computed from the fine (now curved) near wake by interpolation. The results are shown in Fig. 13 which clearly shows the roll up of the tip vortex and the initial roll up of the first center vortex. The sudden jump in displacement between the tip vortex and the center sheet has frequently been observed in experimental investigation.

The next step will involve modifying either the fast free wake model of Ref. 7 or the complete model of Refs. 5 or 6 to include the fine near wake characteristics indicated in Fig. 12 and completing the iteration for blade loads.

SECTION IV FAR WAKE EFFECTS

Another effect requiring more detailed modelling than is possible with the programs of Refs. 5 and 6 is that due to the far wake. In the free wake analyses, the far wake is represented by semi-infinite vortex cylinders whose contributions to the induced velocities at the blade are small. However the influence of these vortex cylinders is more noticeable on the geometry of the intermediate wake and may thereby indirectly affect the induced velocities at the blade. Also it has been pointed out in Ref. 3 that experimental evidence indicates a possible expansion of the wake several spirals below the rotor.

The fast free wake technique of Ref. 7 allows a closer examination of the intermediate wake by the introduction of many more spirals than is feasible with the complete solutions. Fig. 14 shows the standard solution using the vortex cylinder representation for the far wake for the usual two spirals per blade before starting the far wake and for a case with nine spirals which may be expected to bring the far wake sufficiently far away from the blade so as to make its effects negligible. The results show that the solution is essentially independent of the number of spirals, providing at least four are taken in the intermediate wake. Fig. 15 shows the same solution but without the constraint of a fixed far wake. The effect on rotor performance is small as may be expected, but it is interesting to note an expansion of the intermediate wake which may be attributed to the intermingling of the outboard center and tip vortices in a typical Kelvin/Helmholtz instability. Continuation of the solution with more spirals may be expected to show an oscillatory expansion and contraction. Further experimental and analytical investigation of the growth and dissipation of the far wake would appear to be desirable.

SECTION V DEVELOPMENT OF ANALYTICAL TREATMENT

Velocity Induced by a Vortex Ring

As discussed in Section III the roll up of the near wake may be computed by considering the velocities on one element, A, (Fig. 9) of the near wake due to all other elements by treating the spiral wake as a series of vortex rings. This assumption neglects the effects of distortions in those portions of the wake far from the element in question, evidently a reasonable approximation since these distortions are small relative to the radius of the spiral. The relative positions of all elements in the wake in the vicinity of the element A, however, are correctly modelled.

If r is the radius of the vortex ring B of Fig. 9, η is the radial location of A and z is the relative vertical position assumed independent of ϕ (no distortion of the ring) then the vertical component of velocity induced at η due to the vortex ring B is (see, for example, Ref. 24)

$$w = \frac{\Gamma}{4\pi R} \int_0^{2\pi} \frac{r(r - \eta \cos\phi)\, d\phi}{(\eta^2 + r^2 + z^2 - 2r\eta\cos\phi)^{3/2}} = \frac{\Gamma}{4\pi R} I_1$$

With the substitution $\phi = \pi - 2\psi$ such that $\cos\phi = 2\sin^2\psi - 1$

$$I_1 = 2\int_{\pi/2}^{-\pi/2} \frac{-r(r + \eta - 2\eta\sin^2\psi)\, d\psi}{(r^2 + \eta^2 + z^2 - 2r\eta - 4r\eta\sin\psi)^{3/2}}$$

and since the integrand is symmetrical about $\phi = 0$ the integral need be evaluated only from 0 to $\pi/2$. After some manipulation one obtains

$$I_1 = A\int_0^{\pi/2} \frac{d\psi}{(1 - k^2\sin^2\psi)^{3/2}} - B\int_0^{\pi/2} \frac{\sin^2\psi}{(1 - k^2\sin^2\psi)^{3/2}}$$

where $k^2 = \frac{4r\eta}{(r+\eta)^2 + z^2}$ $\quad A = \frac{4r(\eta + r)}{[(r+\eta)^2 + z^2]^{3/2}}$ $\quad B = \frac{8r\eta}{[(r+\eta)^2 + z^2]^{3/2}}$

These integrals may be evaluated by standard methods for complete elliptic intervals of the first kind

$$K = \int_0^{\pi/2} \frac{d\psi}{(1 - k^2\sin^2\psi)^{1/2}}$$

and second kind

$$E = \int_0^{\pi/2} (1 - k^2\sin^2\psi)^{1/2}\, d\psi$$

noting that

$$\frac{1}{(1 - k^2\sin^2\psi)^{3/2}} = (1 - k^2\sin^2\psi)^{1/2} + \frac{k^2\sin^2\psi}{(1 - k\sin^2\psi)^{3/2}} + \frac{k^2\sin^2\psi}{(1 - k^2\sin\psi)^{1/}}$$

and $\frac{dK}{dk} = \int \frac{k\sin^2\psi\, d\psi}{(1 - k^2\sin^2\psi)^{3/2}} = \frac{1}{k}\left(\frac{E}{1 - k^2} - K\right)$

$$\frac{dE}{dk} = -\int \frac{k\sin^2\psi}{(1 - k^2\sin^2\psi)^{1/2}}\, d\psi = \frac{1}{k}(E - K)$$

Hence $$I_1 = A \times \frac{E}{(1 - k^2)} - \frac{B}{k^2}\left(\frac{E}{1 - k^2} - K\right)$$

which, after substitution for A and B becomes

$$I_1 = \sqrt{\frac{k^2}{r\eta}}\left[K - E\left[1 - .5k^2(1 + r/\eta)\right]/(1 - k^2)\right]$$

from which w may be evaluated for any value of k.

In the absence of a computer with a library of elliptic functions it is convenient to use series solutions for E and K. The most suitable for the present application are Cayley's logarithmic series because of their rapid convergence, although care must be taken in the vicinity of $k^2 \longrightarrow 1$.

From Ref. 25, 777.3 and 777.4, and defining

$$F = \ln\left(\frac{4}{\sqrt{1 - k^2}}\right),$$

$$E = 1 + .5(F - .5)(1 - k^2) + \frac{3}{16}\left(F - 1 - \frac{1}{12}\right)(1 - k^2)^2 + \cdots$$

$$K = F + .25(F - 1)(1 - k^2) + \frac{9}{64}\left(F - 1 - \frac{1}{6}\right)(1 - k^2)^2 + \cdots$$

The radial component of induced velocity at η is

$$u = \frac{\Gamma}{4\pi R} \int \frac{z\, r \cos\phi \, d\phi}{(\eta^2 + r^2 + z^2 - 2r\eta \cos\ )^{3/2}}$$

which, following the same procedure used above may be evaluated as

$$u = \frac{\Gamma}{4\pi r} \cdot \frac{z}{2\eta}\sqrt{\frac{k^2}{r\eta}}\left[E(2 - k^2)/(1 - k^2) - 2K\right]$$

A self induced velocity will exist on the curved vortex, which from Ref. 26, may be expressed as

$$ws = \frac{\Gamma}{4\pi R}\left[\ell n(8r/\Delta r) - \frac{1}{4}\right]$$

where Δr is the core radius. Ref. 27 suggests a value of $\frac{\Delta r}{r}$ of .025 as typical for helicopter rotor loadings. The experimental results of Ref. 21 indicate that $\frac{\Delta r}{r}$ could vary from .01 to .03, depending on the proximity of the vortex to first encounter, hence the term in brackets could vary from about 5.5 to 6.2. Since the singularity is logarithmic, and the contribution of the self induced velocities is small, the solution is not sensitive to an exact definition of $\frac{\Delta r}{r}$. A value of $ws = \frac{\Gamma}{4\pi R}[6]$ has been used for all the cases of Fig. 12.

In Ref. 7 it was shown that the drop off of bound circulation at the tip of a rotor blade may be closely approximated by an expression of the form

$$\frac{\Gamma(\eta)}{\Gamma_0} = (1 - \eta^2)^{1/3}$$

which has been used in determining the strength of the trailing vortex system for the computation of the tip vortex roll up of Fig. 10. However in the case of Fig. 13, the computed bound circulation distribution has been used.

Effect of Bound Circulation

In order to examine possible effects of the bound circulation on the near wake displacements, a simple case of two parallel infinite blades of chord b operating in a wind stream of velocity V and subjected to a uniform downwash u_0 will be considered, but with the blades treated as airfoils, or lifting surfaces, rather than lifting lines, since the effects of the bound circulation are expected to be of importance primarily in the vicinity of the surfaces themselves.

The bound circulation may be represented by a series (see, for example, Ref. 19,), of the form

$$\gamma(x) = A_0 \cot \frac{\theta}{2} + \sum_{n=1}^{\infty} A_n \sin n\theta$$

where $x = \frac{b}{2}(1 - \cos \theta)$.

The velocity induced on the airfoil by the element of vorticity $\gamma(x)dx$ is

$$v(x) = \frac{A_0}{2} + \sum \frac{A_n}{2} \cos n\theta$$

For a flat airfoil in steady flow, only A_0 is nonzero.

It is desired to find the displacement of any element in the wake between the airfoils when both are at an angle of attack α.

Boundary conditions on the blade require that, for α,

$$v(x) = V\alpha$$

everywhere on the blade whence

$$A_0 = 2V\alpha$$

and, since $\cot\theta = \frac{\sin\theta}{1 - \cos\theta}$

$$\gamma(x) = 2V\alpha \frac{\sin\theta}{1 - \cos\theta}$$

$$= 2V\alpha\sqrt{\frac{b - x}{x}}$$

Referring to Fig. 16, the velocity at any distance ξ behind the first airfoil, and $p - \xi$ ahead of the second airfoil, due to an element of bound vorticity $\gamma(x)$ on each airfoil is

$$\Delta u = \frac{\gamma(x)dx}{2\pi}\left[\frac{\xi + b - x}{(\xi + b - x)^2 + z^2} - \frac{p - \xi + x}{(p - \xi + x)^2 + z^2}\right]$$

If a steady uniform velocity u_0 exists perpendicular to the airfoils, for example from the rest of the wake, then the vertical velocity at ξ is

$$\frac{dz}{dt} = \sum\Delta u + u_0$$

or, since $\frac{d\xi}{dt} = V$

$$dz = \left[\sum\frac{\Delta u}{V} + \frac{u_0}{V}\right] d\xi$$

whence

$$z = \sum_{\xi=0}^{\xi=p}\left\{\sum_{x=0}^{x=b}\frac{\alpha}{\pi}\sqrt{\frac{b - x}{x}}\left[\frac{b + \xi - x}{(b + \xi - x)^2 + z^2} - \frac{p - \xi + x}{(p - \xi + x)^2 + z^2}\right]dx + \frac{u_0}{V}\right\} d\xi$$

which may be readily programmed for direct numerical integration. Fig. 11 shows the results obtained for the case of $\alpha = .1$ radians on both airfoils. Evidently the displacements are everywhere small, and essentially zero at the second airfoil. Fig. 11c shows the displacements when $u/V_0 \equiv \lambda_0$ has a typical value of .02.

The actual conditions could of course differ from those of the simplified model used here. The bound circulation varies along the blade and particularly near the tip. The trailed tip vortex moves rapidly inboard and therefore may encounter a slightly different velocity field due to the bound circulation near the second blade. In order to examine the extreme of such a condition Fig. 11c shows the case where the bound circulation on the second airfoil was set equal to zero. The solution then reverts to the familiar case of the downwash behind a lifing airfoil. The z displacements are still small, of the order of 20% of the vertical displacement at first encounter for a two bladed rotor. The bound circulation has been included in the models used in Volumes II and III, although its effect was found to be negligible. Its neglect in the simplified solutions of Section III appears to be a reasonable approximation.

SECTION VI

Conclusions

1) Free wake techniques of varying complexity have been developed for predicting airloads on rotor blades, all of which agree well with experimental observation of both the bound circulation distribution and wake geometry.

2) Simplified models in which velocities are computed only in the wake directly behind each blade and averaged to obtain wake displacements give results in agreement with the more complete solutions in which wake velocities are computed everywhere in the near and intermediate wakes.

3) Techniques have been developed for predicting the migration of the tip vortex in the near wake for the complete solution, however uncertainties as to the exact roll up mechanism and near wake geometry still remain.

4) An analysis of the roll up mechanism in the near wake using a simplified model which permits use of a fine trailing wake indicates that roll up of the tip vortex is essentially completed in a few chord lengths behind a blade.

5) The vertical displacement of the centroid of vorticity in the near wake depends on the assumed core size (artificial viscosity) of the vortex filaments representing this wake and the solutions became chaotic for small or zero values of core size.

6) Use of a rigid far wake has little effect on the predicted blade loads but does affect the geometry of the intermediate wake.

7) Effects of bound vorticity on near wake displacements are negligible and its neglect in the simplified solution is justified.

Recommendations

1) Extend either the simplified or more detailed solutions to include a more complete representation of the near wake vortex roll up and iterate for a final converged solution using this more complete wake geometry.

2) Develop more formal techniques for including the effects of viscosity in the determination of wake geometry.

3) Extend the solution to include a lifting surface representation of the blade for use with rotors having four and more blades and in order to allow for the effects of spanwise flow along the blade.

4) Obtain experimental verification of blade bound vorticity distribution and wake geometry for rotors with four and more blades.

REFERENCES

1 R.B. Gray et al., "Helicopter Hovering Performance Studies," Princeton Univ. Aero Eng. Report 313, 1955.

2 A.J. Landgrebe, "An Analytical and Experimental Investigation of Helicopter Rotor Hover Performance and Wake Geometry Characteristics," USAAMRDL TR71-24, 1971.

3 J.D. Kocurek and L.F. Berkovitz, "Velocity Coupling - A New Concept for Hover and Axial Flow Wake Analysis and Design," AGARD-CPP-344, April 1982.

4 J.D. Ballard, K.L. Orloff and A. Luebs, "Effect of Tip Shape on Blade Loading Characteristics and Wake Geometry for a Two-Bladed Rotor in Hover," Journal of the American Helicopter Society, Vol. 25, No. 1, pp. 30-35, January 1980.

5 A. Tanuwidjaja, "Free Wake Techniques for Rotor Aerodynamic Analysis, Volume II: Vortex Sheet Models," ASRL Report 199-2, December 1982.

6 M. Brower, "Free Wake Techniques for Rotor Aerodynamic Analysis, Volume III: Vortex Filament Models," ASRL Report 199-3, December 1982.

7 R.H. Miller, "Simplified Free Wake Analyses for Rotors," FFA (Sweden) TN 1982-7; also MIT ASRL TR 194-3.

8 J.D. Cohard, "Free Wake Analysis of Wind Turbine Aerodynamics," U.S. Dept. of Energy COO 3141-T1; also MIT ASRL TR 194-14, September 1978.

9 Letter Progress Report, Feb. 10, 1981, Contract NAG2-47.

10 R.H. Miller and A. Tanuwidjaja, "Interim Progress Report, Development of Analytical Techniques for Rotor Aerodynamic Analysis," MIT ASRL TR 194-6, January 1982.

11 W. Johnson, "Comparison of Calculated and Measured Model Rotor Loading and Wake Geometry," NASA TM 81189, April 1980.

12 F.X. Caradonna and C. Tung, "Experimental and Analytical Studies of a Model Helicopter Rotor in Hover," Proceedings of 6th European Rotorcraft and Powered Lift Forum, September 1980.

13 R.H. Miller, "A Simplified Approach to the Free Wake Analysis of a Hovering Rotor," Vertica, Vol. 6, pp. 89-95, 1982.

14 R.H. Miller, "Rotor Hovering performance Using the Method of Fast Free Wake Analysis," AIAA-82-0094, January 1982 (to be published AIAA JAC).

15 M. Scully, "Computation of Helicopter Rotor Wake Geometry and Its Influence on Rotor Harmonic Airloads," MIT ASRL TR 178-1, March 1975.

REFERENCES, Continued

16 N. Ham, "Some Conclusions from an Investigation of Blade-Vortex Interaction," Journal of the Americal Helicopter Society, Vol. 20, No. 4, pp. 26-31, October 1975.

17 R.H. Miller, "Application of Fast Free Wake Analysis Techniques to Rotors," Proceedings of 8th European Rotorcraft and Powered Lift Forum, August 31 through September 3, 1982.

18 F.L. Westwater, Aero Res. Council, R and M, No. 1962, 1935

19 G.K. Batchelor, AN INTRODUCTION TO FLUID DYNAMICS, C.U. Press, 1967.

20 G.R. Baker, "The 'Cloud in Cell' Technique Applied to the Roll Up of Vortex Sheets," Journal of Computational Physics 31, pp. 76-95, 1979,

21 E.M. Murman and P.M. Stremel, "A Vortex Wake Capturing Method for Potential Flow Calculations," AIAA Paper 82-0947, June 1982.

22 P.M. Stremel, "Computational Method for Non-Planar Vortex Wake Flow Fields with Applications to Conventional and Rotating Wings," M.S. thesis, Department of Aeronautics and Astronautics, MIT, Cambridge, Mass, February 1982.

23 T.C. Biggers, A. Lee, K.L. Orloff and O.T. Lemmer, "Measurements of Helicopter Rotor Tip Vortices," American Helicopter Society Forum Proceedings, May 1977.

24 R.H. Miller, "Blade Harmonic Airloading," AIAA Journal, July 1964.

25 H.B. Dwight, TABLES OF INTEGRALS AND OTHER MATHEMATICAL DATA, MacMillan 1961.

26 H. Lamb, HYDRODYNAMICS, Dover, 1945.

27 M.T. Landahl, "Roll-up Model for Rotor Wake Vortices," FFA (Sweden) HU-2262-Pt. 5-1981. Also MIT ASRL TR 194-4.

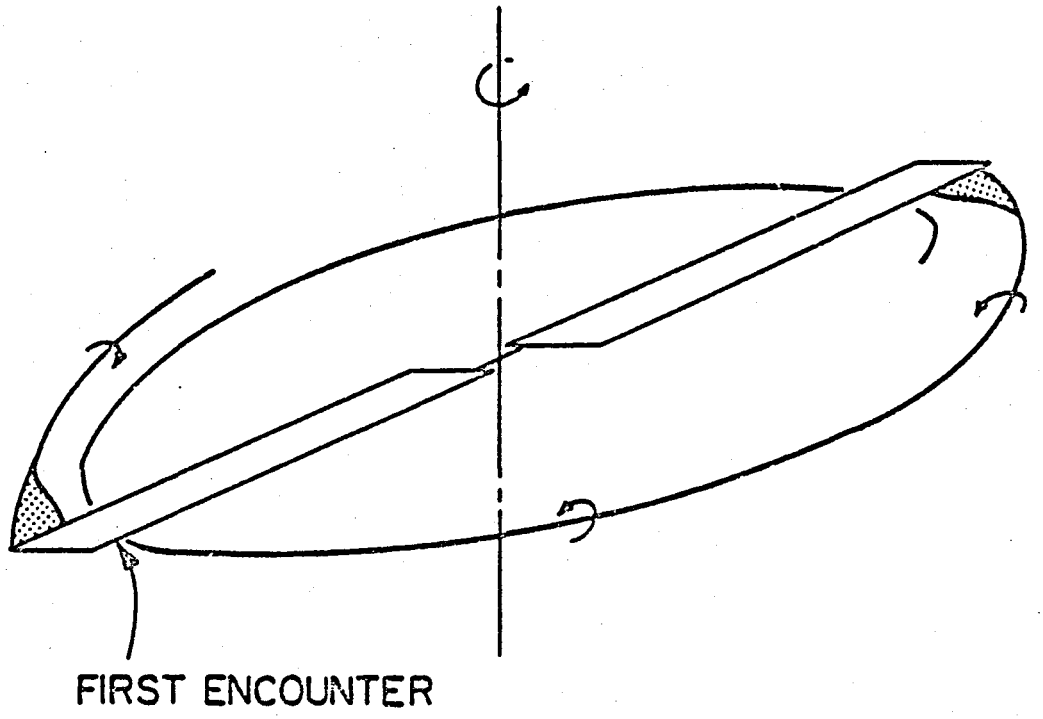

Fig. 1 Geometry of first blade vortex encounter.

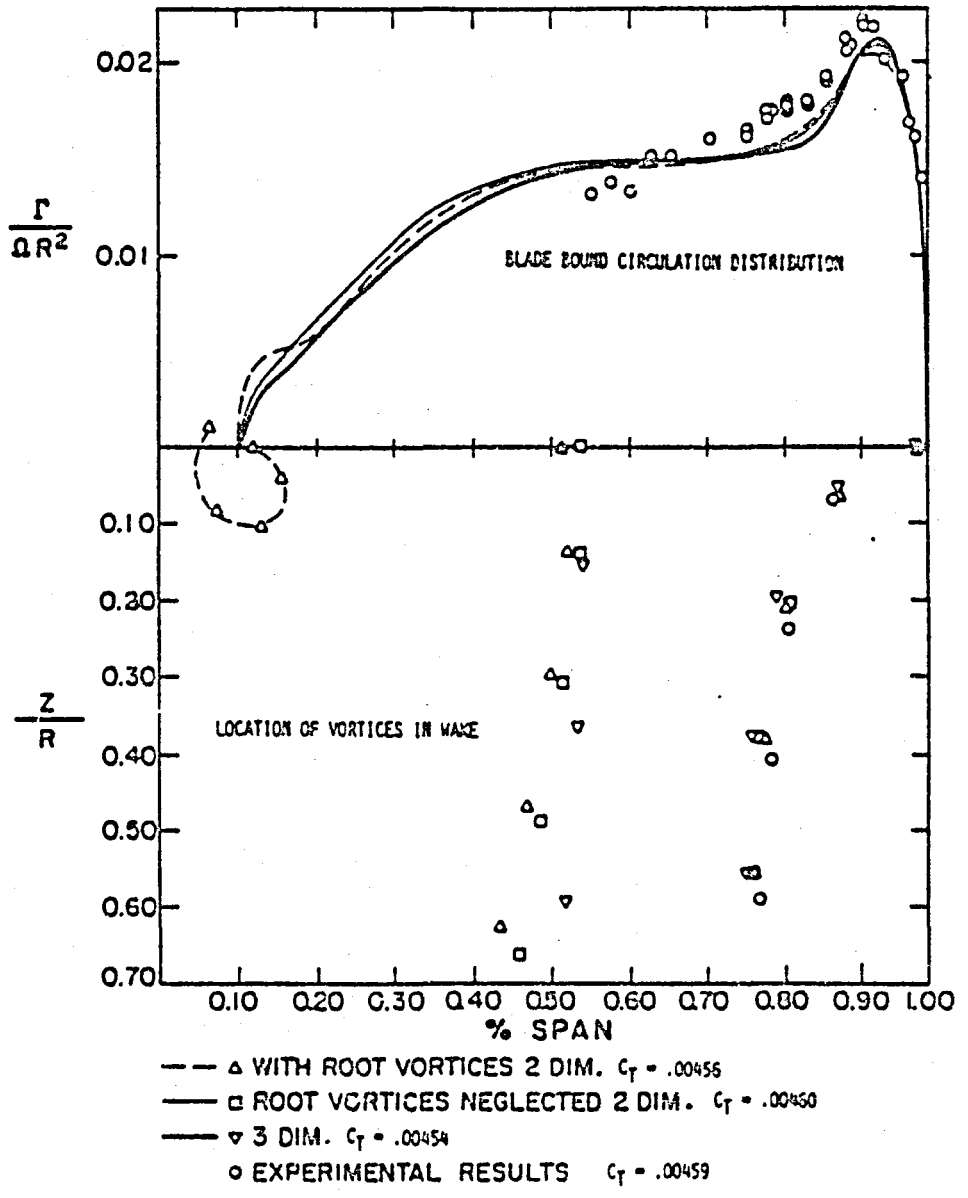

Fig. 2 Blade bound vortex distribution and wake geometry as predicted by methods of Ref. 7 compared with experimental results of Refs. 4 and 11.

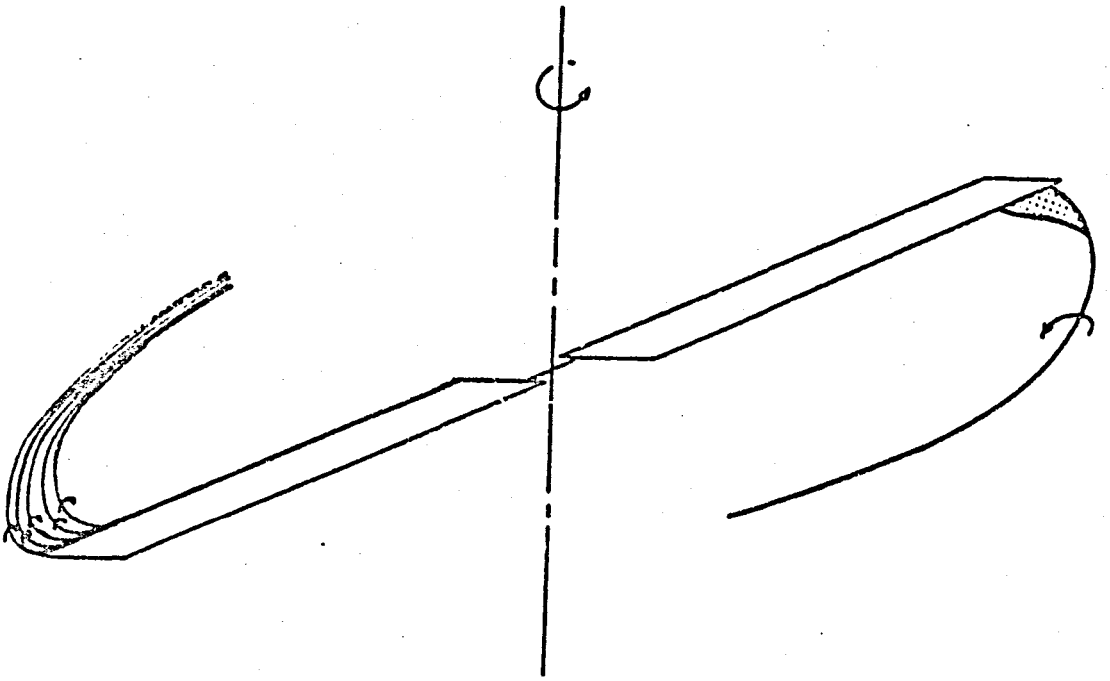

Fig. 3 Representation of trailed vorticity from blade tips by series of vortex filaments.

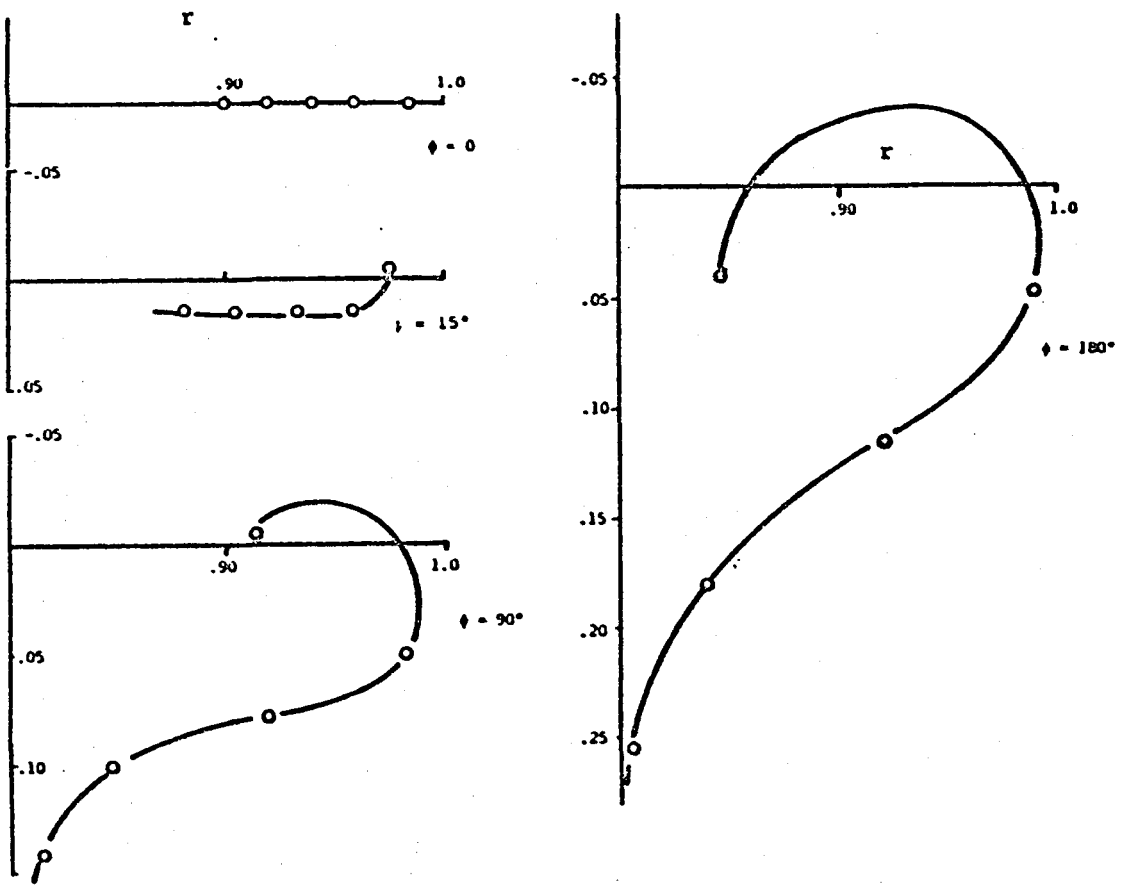

Fig. 4 Roll up of tip vortex as predicted by full vortex sheet model of Ref. 5.

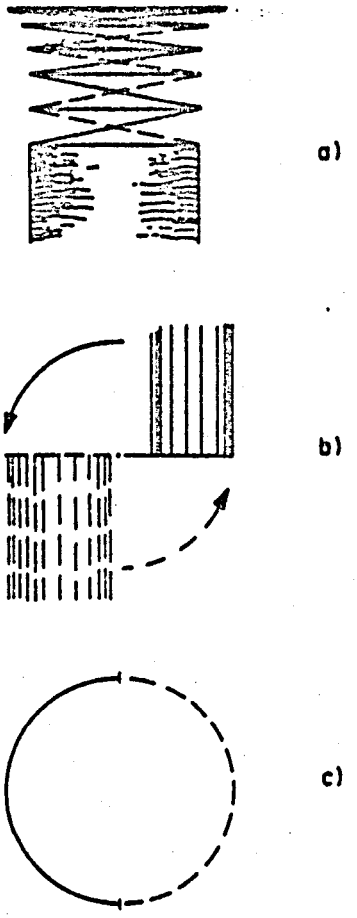

Fig. 5 Geometry of model using vortex rings and cylinders to represent the wake.

a) Side view of rotor wake model showing intermediate and far wakes formed from vortex spiral - 2 blades. Tip vortex only shown.

——— Blade One — — — Blade Two

b) Plan view showing near wake

c) Formation of intermediate wake

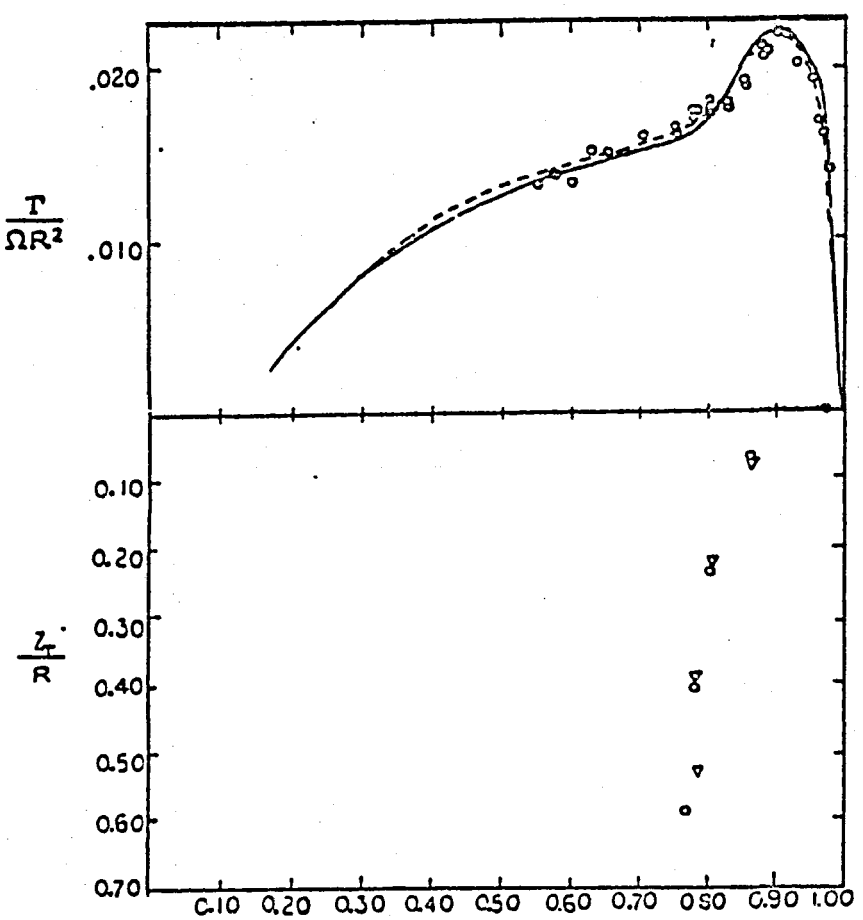

Fig. 6 Final results from complete wake model of Ref. 5 showing effect of different roll up schedules on the bound circulation and wake geometry.

------- Outboard center vortex rolled up from peak to 82.5%

——— Outboard center vortex rolled up from peak to 71.5%

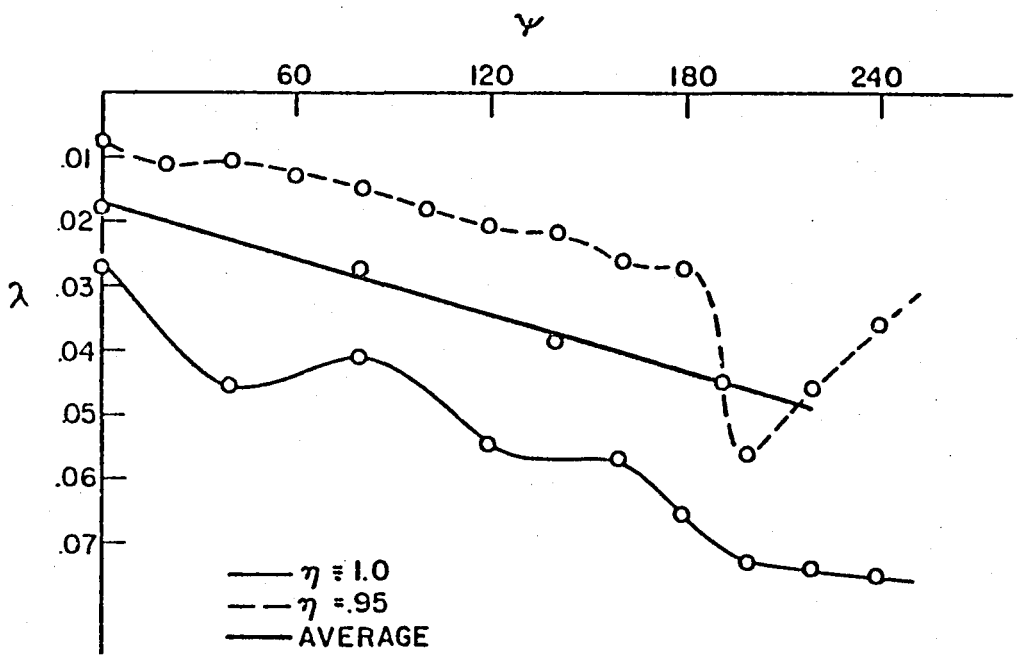

Fig. 7 Typical distribution of vertical velocities in near wake using full vortex sheet model results of Ref. 9. The heavy line averages the velocities at $\eta = 1.0$ and $\eta = .95$.

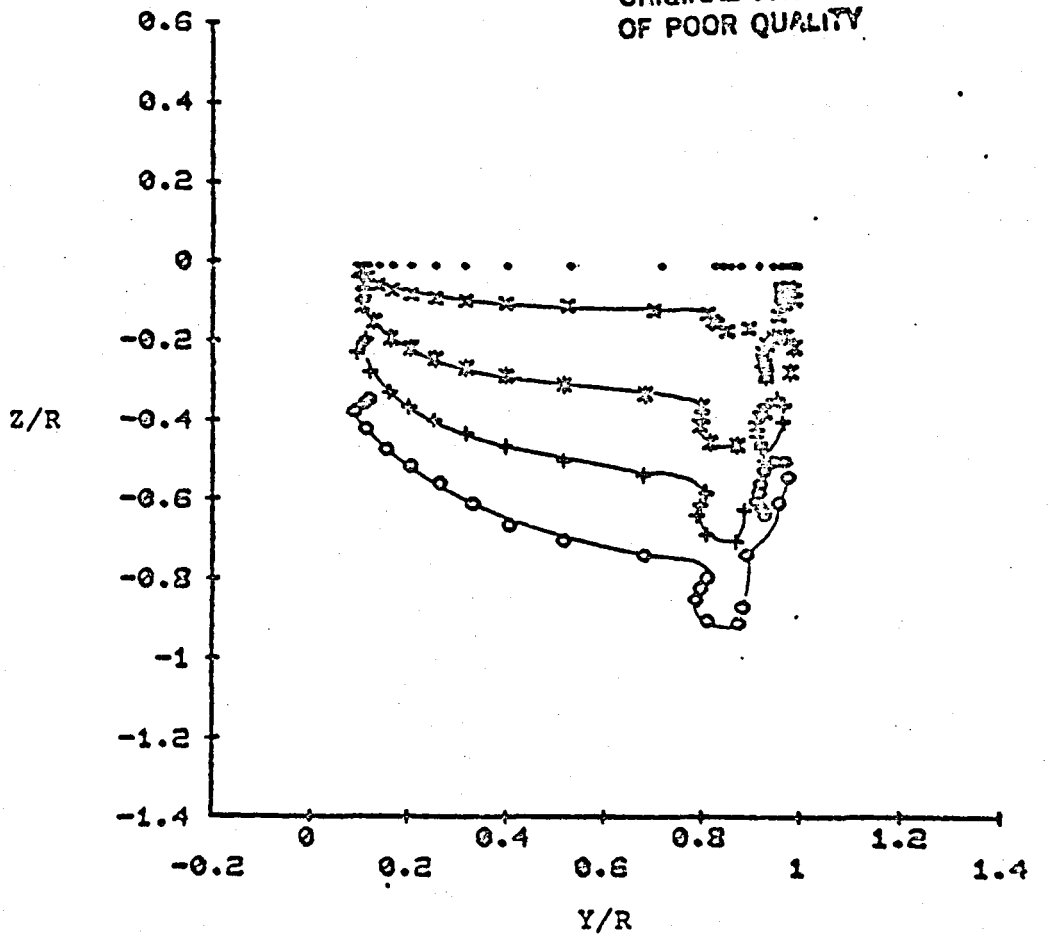

Fig. 8 Wake displacements obtained from Euler Lagrange solutions of Ref. 22.

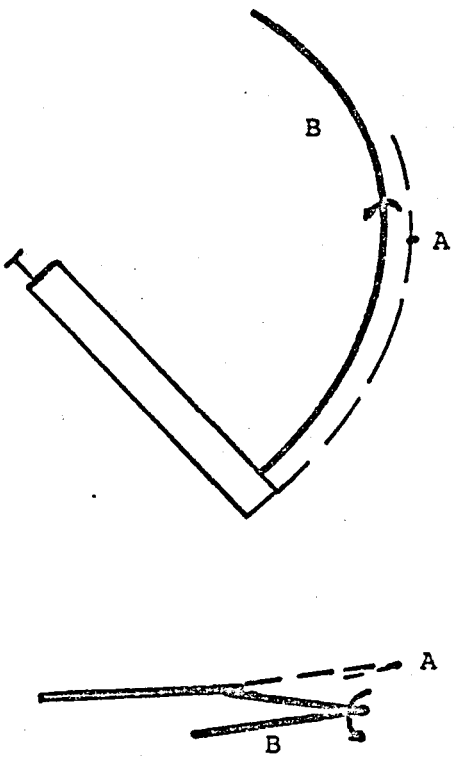

Fig. 9 Geometry of near wake roll up model.

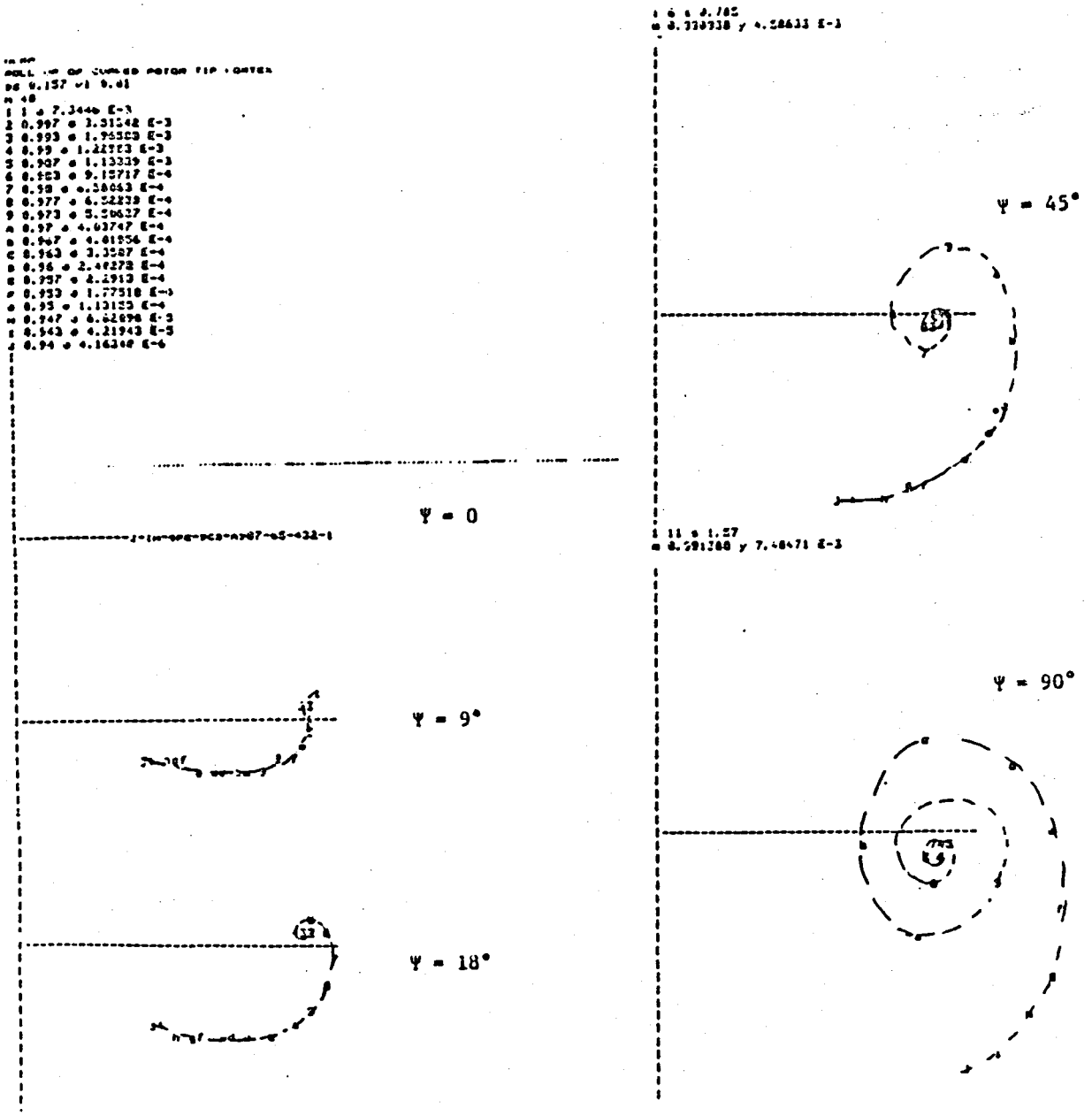

Fig. 10 Predicted roll up of tip vortex - near wake only considered.

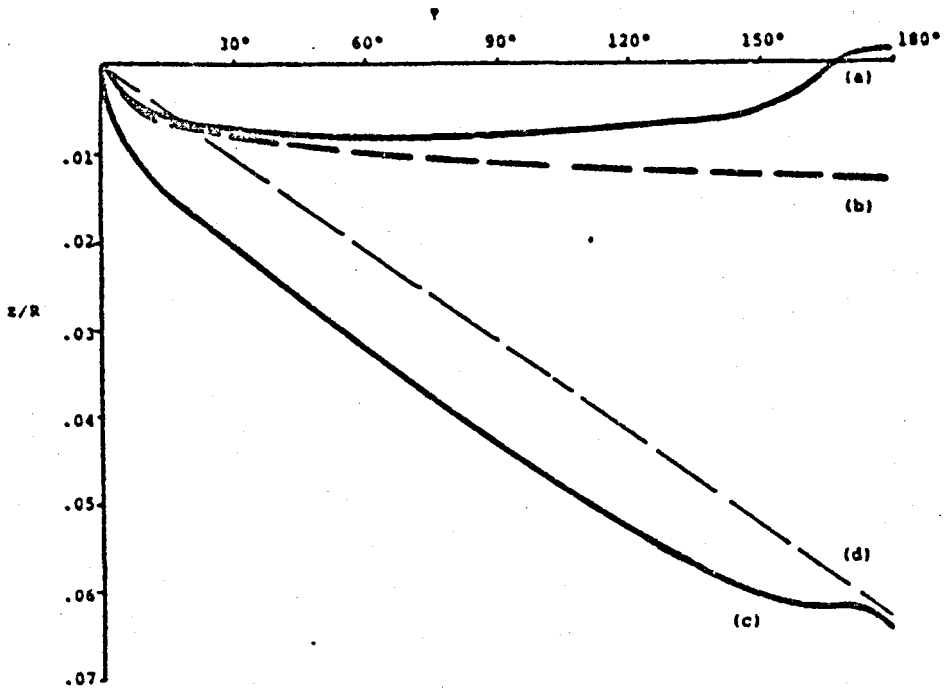

Fig. 11 Effect of bound circulation on vortex migration between two lifting surfaces.

(a) Effects of bound circulation only from both surfaces

(b) Same but with bound circulation on originating surface only

(c) Same as (a) but including a steady inflow of $\lambda = .02$

(d) Effect of steady inflow $\lambda = .02$ without bound circulation

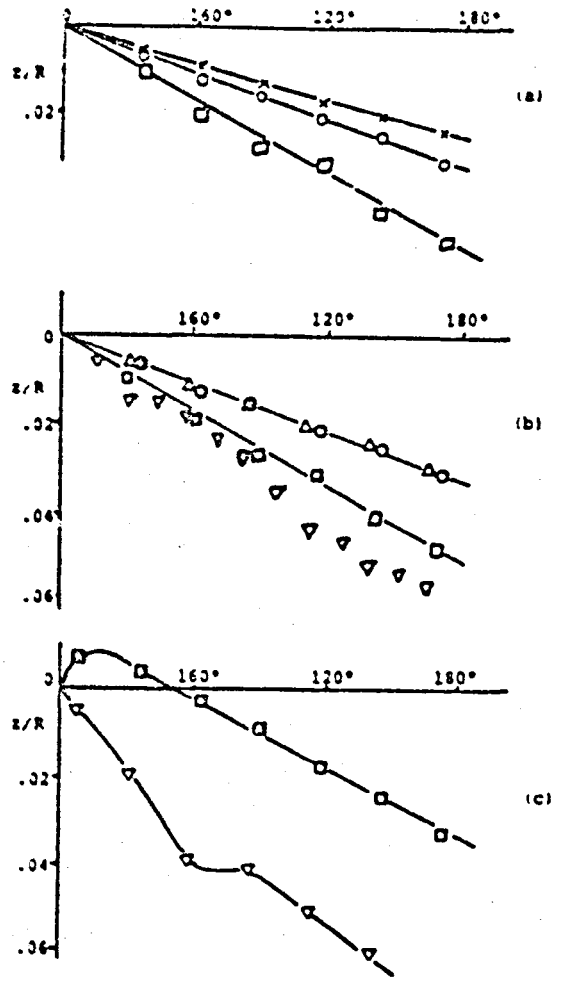

Fig. 12 Effect of core size and interval size on migration of tip vortex centroid in near wake, ϕ = 0 to 180°.

(a) Effect of core size

x .02R o .01R □ .002R

(b) Effect of interval size

o $\Delta\Psi$ of .05π Core size of .01R

Δ $\Delta\Psi$ of .025π Core size of .01R

□ $\Delta\Psi$ of .05π Core size of .002R

▽ $\Delta\Psi$ of .025π Core size of .002R

(c) Effect of interval size for core size of zero

□ $\Delta\Psi$ = .05π ▽ $\Delta\Psi$ = .025π

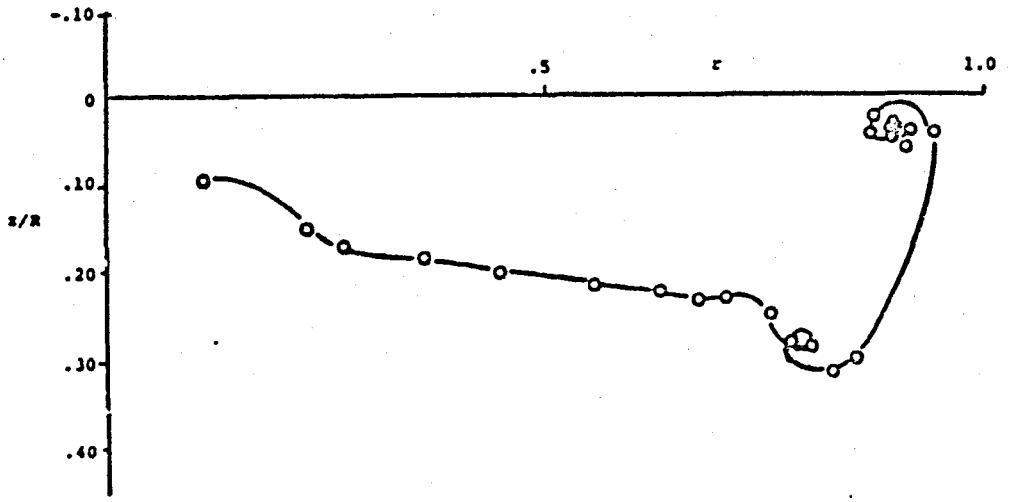

Fig. 13 Roll up of near wake for case of Fig. 2 at $\Psi = 180°$ including intermediate and far wake effects. Core size of .01R. Interval size $\Delta\Psi = .05\pi$.

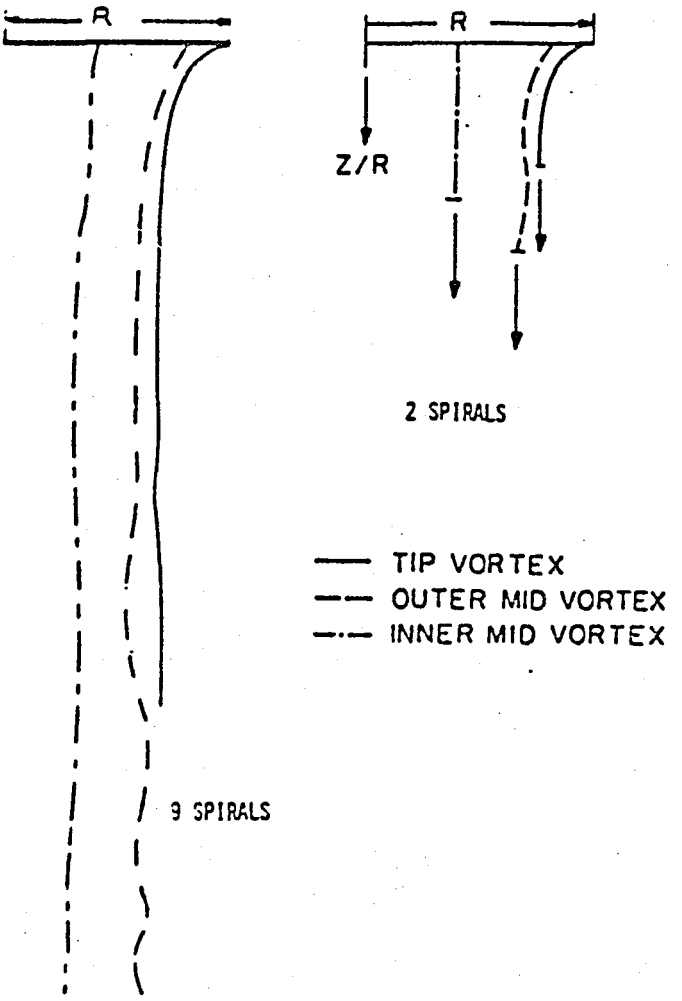

Fig. 14 Effect of extent of intermediate wake with far wake.
2 spirals C_T = .00456 9 spirals C_T = .00454

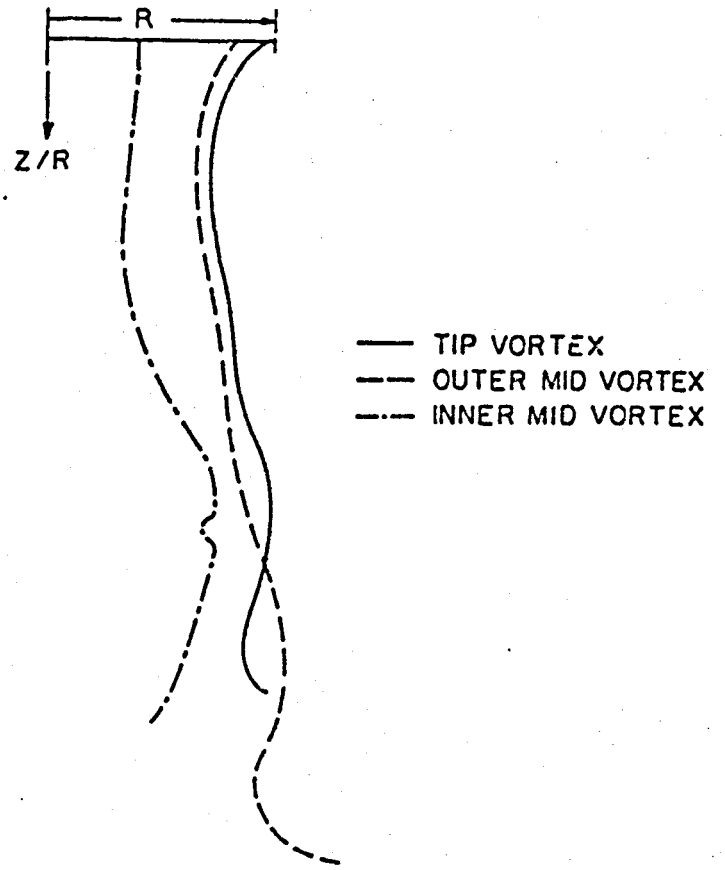

Fig. 15 Effect of eliminating far wake with extended intermediate wake.
9 spirals $C_T = .0044$

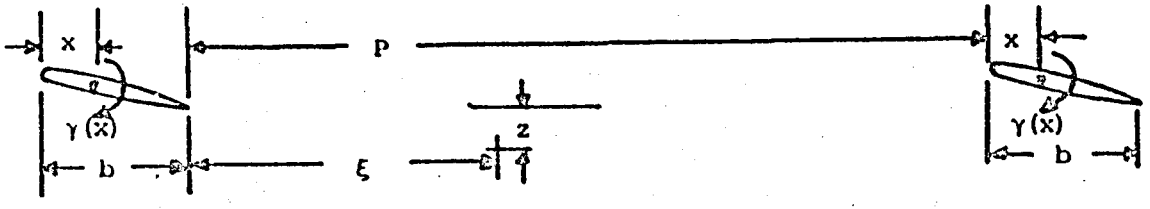

Fig. 16 Model for studying effect of bound circulation from two lifting surfaces on wake displacements.